

Monte Carlo simulation of a lyotropic first-order isotropic-nematic phase transition in a lattice polymer model

H. Weber, W. Paul,* and K. Binder

Institut für Physik, Johannes-Gutenberg-Universität, Staudingerweg 7, D-55099 Mainz, Germany

(Received 17 June 1998)

We present a Monte Carlo simulation of the bond-fluctuation lattice model, using a Hamiltonian which introduces a change in the conformational statistics of the polymer chains from Gaussian behavior at high temperatures to rigid rod behavior at low temperatures. We do not introduce any attractive interaction between the chains. Upon cooling, the aspect ratio of the chains increases above the critical value for the density employed in the simulation, and we observe an entropically driven phase transition into a nematic phase. We examine this transition quantitatively by a careful finite size scaling study using an optimized cumulant intersection method, and show that the transition is of first order. [S1063-651X(99)12302-X]

PACS number(s): 61.25.Hq, 61.20.Ja, 61.30.-v, 64.70.Md

I. INTRODUCTION

Changing the stiffness and concentration of semiflexible polymers in solution can introduce a rich liquid crystalline phase behavior [1–4]. Understanding and predicting this phase behavior in terms of the intramolecular and intermolecular interactions of the chains is at the same time of high technological importance and a large fundamental challenge. If the polymer chains, or, in the limit of infinite stiffness, the rigid rodlike molecules, interact through orientation-dependent attractive interactions which favor a parallel alignment of the molecules [5], it is easy to visualize a transition from an isotropic solution at low concentrations to a nematically ordered solution at high concentrations. The molecules can lower their interaction energy upon ordering into the nematic phase, and we obtain a so-called thermotropic nematic phase transition [6,4]. Since the pioneering work of Onsager [7], we know, however, that an isotropic-nematic transition can also occur if there are only repulsive excluded volume interactions between the molecules. In this case the transition is completely driven by the behavior of the entropy. The molecules lose orientational entropy upon ordering, but they gain translational entropy and this drives the phase transition. The theory of this so-called lyotropic nematic phase transition, for instance, predicts that the value of the orientational order parameter at the transition should depend on the density in contrast to the purely thermotropic case. This has also been seen experimentally [8,9], which shows that excluded volume effects also play a role in this phase transition in real systems.

All theoretical treatments of the isotropic-nematic transition [10–14] of continuum models for semiflexible polymers predict a first-order phase transition. This transition has been analyzed by computer simulations [15,16], and in Ref. [16] it was shown that the analytical calculations not only provide a qualitative description of the coexistence densities of the isotropic and nematic phase but are also able to predict the transition densities to within about 20%.

For lattice polymer models the situation is different. The

theoretical analysis started with the work of Flory [17], whose theory predicted a first-order isotropic-nematic phase transition when the flexibility of the lattice polymer chains decreases below a certain threshold. It could, however, be shown that Flory's approximation of the configurational entropy of the polymer chains is too drastic [18–21], and that in an improved treatment the transition is removed to infinite stiffness. This agrees with the findings of lattice model simulations of the isotropic-nematic transition [22,23], which showed no phase transition but the occurrence of nematically ordered domains of a size corresponding to fully stretched chains. Only through an introduction of aligning interactions between the chains could a phase transition be induced. All these observations are completely at odds, however, with exactly solvable very simplified lattice polymer models [24,25] which show a second-order phase transition into the nematic phase. From this comparison it is clear that the occurrence and type of the isotropic-nematic phase transition in lattice polymer models depend strongly on the details of the model (and the underlying lattice), which influence the subtle interplay between translational and orientational entropy that determines this phase transition.

In the remainder of this paper we will show that the bond-fluctuation lattice model with a suitably chosen Hamiltonian, that leads to an increasing stiffness of the chains upon cooling but does not contain any attractive interactions between the chains, indeed possesses a first-order phase transition from an isotropic to a nematic phase. A typical snapshot of the order in the nematic phase is shown in Fig. 1. In Sec. II we will define the model and the simulation technique. Section III will present some theoretical background on the finite size scaling analysis of a nematic phase transition. In Sec. IV we will discuss our results and present some conclusions.

II. MODEL

In this study we use the three-dimensional version of the bond-fluctuation lattice model, which has been discussed in detail in the literature [26,27]. Each monomer occupies the eight corners of a unit cube on the simple cubic lattice, i.e., its size is $V=2^3$ in units of the lattice constant. The bonds connecting the monomers are generated out of the set B

*Electronic address: Wolfgang.Paul@uni-mainz.de

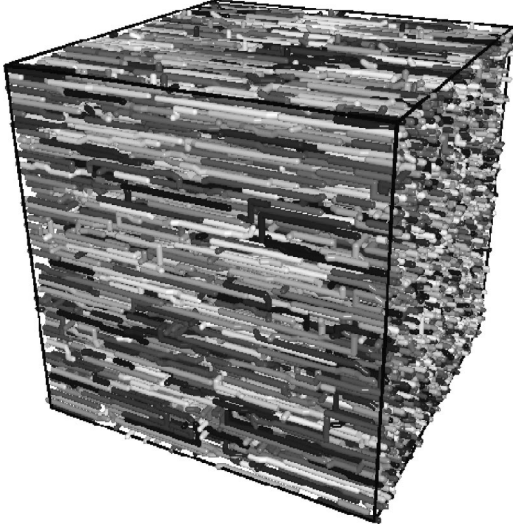


FIG. 1. Configuration snapshot for a system of chains of length $N=20$ at a temperature $T=0.219$ in the nematic phase.

$=\{(2,0,0), (2,1,0), (2,1,1), (2,2,1), (3,0,0), (3,1,1)\}$ by all possible lattice symmetry operations. The shortest bond length puts two monomers adjacent to each other on the lattice. Two monomers whose centers are connected by the largest bond length are still so close that no other monomer can pass between them (chain connectivity). Temperature is introduced by the Hamiltonian

$$H(\{b\}, \{\theta\}) = \sum_{\{b\}} \epsilon_b (b - b_0)^2 + \sum_{\{\theta\}} \epsilon_\theta \cos(\theta) (1 + c_0 \cos(\theta_0)), \quad (1)$$

which contains only intramolecular degrees of freedom. $\{b\}$ denotes the set of all bond lengths, and $\{\theta\}$ denotes the set of all bond angles. $\epsilon_b = 1$ defines the energy scale of the model (temperatures will henceforth be given in units of ϵ_b), and we choose $\epsilon_\theta = 0.67$, $b_0 = 0.86$, and $c_0 = 0.03$ [28]. The Hamiltonian therefore favors short bond lengths ($b_{\min} = 2$) and stretched bond angles ($\theta = \pi$). At high temperatures these chains are known to conform to the Gaussian statistics of polymer chains in the melt [26,27], and the ground state of each chain is a rigid rod with all bonds collinear and of type $(2,0,0)$. The contour length of the chains in the ground state is $2N$ lattice units, and its width is that of a monomer, i.e., $d=2$. The variation of the chain stiffness as a function of temperature can be seen in Fig. 2, where we show the characteristic ratio of the chains of length $N=20$:

$$C_N = \frac{\langle R^2 \rangle}{(N-1)\langle l^2 \rangle}, \quad (2)$$

where $\langle R^2 \rangle$ is the mean squared end-to-end distance of the chains, N is the degree of polymerization, and $\langle l^2 \rangle$ is the mean squared bond length. The characteristic ratio strongly increases toward its ground state value of $C_N = 19$ for temperatures below $T = 0.3$, giving us a first indication where to expect the nematic ordering phenomenon.

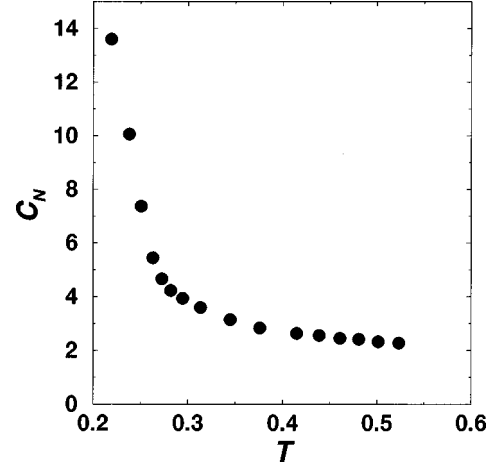


FIG. 2. Chain stiffness as measured by the characteristic ratio as a function of temperature for the chains of length $N=20$. The definition is given in the text. We observe a sharp increase in stiffness for temperatures $T < 0.3$.

The intermolecular interaction in the model is pure excluded volume interaction, realized in the lattice model by prohibiting double occupancy of lattice sites. This model has been used previously in studies of the free volume percolation transition in polymer matrices [29] and the excess scattering induced by intramolecular ordering of these chains upon cooling [30]. We will discuss simulations performed at a constant polymer volume fraction of $\Phi = 0.5$ and for chains of length $N=20$, with some results also presented for chains of length $N=10$ for comparison.

At low temperatures a Monte Carlo simulation using Metropolis rates exhibits an exponentially decreasing acceptance rate, and we are addressing an ordering phenomenon with an algebraic (second order) or rounded algebraic (first order) divergence of relaxation times near the transition temperature. Furthermore, we have to simulate rather large systems to allow for the occurrence of differently oriented nematic domains and to be able to perform a finite size scaling study using the subensemble method [31]. In this study the largest linear dimension of the system was $L = 130$. One important technical advantage of the bond-fluctuation model at this volume fraction is the ability of the slithering snake reptation algorithm (see Refs. [32,33] for a version of this algorithm that allows for further dynamic simulations using a random hopping algorithm [27]) to equilibrate the simulated system through the whole transition region. Despite the fact that our system size $L = 130$ means that we have almost 1.1 million monomers in the system, times of order 10^7 Monte Carlo steps (MCS) per monomer can be reached. To check equilibration and exclude the occurrence of frozen-in metastable states, we performed stepwise cooling from the melt for the temperatures $T = 0.367, 0.282, 0.263$, and 0.251 , and stepwise heating from a columnar crystal for $T = 0.219, 0.238, 0.251$, and 0.263 . For the two temperatures where completely different starting configurations were used, Fig. 3 shows that we were well able to equilibrate the structures and that there are no discernible effects of the thermal history of the sample. Comparing the behavior of the mean squared end to end distance of the chains in Fig. 3(a) to the order parameter of the system (which will be defined in Sec. III) in Fig.

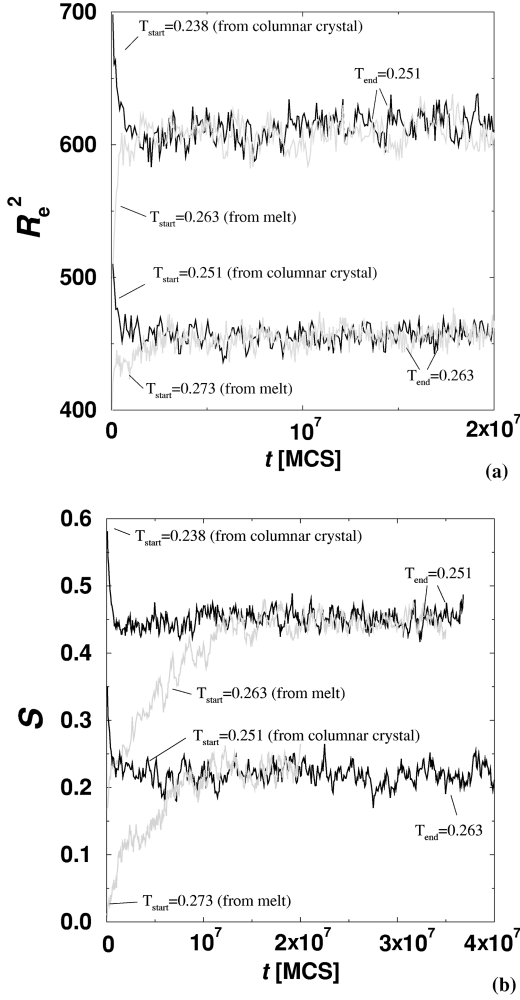


FIG. 3. (a) Equilibration time series for the mean squared end-to-end vector for two different simulation temperatures T_{end} . For both temperatures time series starting from a columnar crystal at lower temperature and a melt configuration at higher temperature are shown. Both time series reach the same equilibrium value at about 10^6 Monte Carlo time units. (b) Same as (a) for the nematic order parameter. Here the equilibration time is about 10^7 Monte Carlo time units.

3(b), we furthermore note that the latter needs about an order of magnitude more simulation time for equilibration. Figure 3(b) also indicates that the two temperatures shown lie in the nematic region of the phase diagram, which will be demonstrated in Sec. IV.

III. HOW TO ANALYZE THE ISOTROPIC-NEMATIC TRANSITION

In the nematic phase the orientational isotropy of the system is broken, and the molecules are preferentially oriented along some direction called the nematic director \hat{n} . The global nematic order parameter can be defined as the expectation value of the second Legendre polynomial of the inner product of a unit vector \hat{u}_i characterizing the molecular orientation and the nematic director:

$$S = \frac{1}{2} (3 \langle (\hat{u}_i \cdot \hat{n})^2 \rangle - 1). \quad (3)$$

The unit vector \hat{u}_i is taken along the symmetry axes of a molecule [34–37] (not available here), the principal axes of inertia of a polymer [15], or the individual polymer segments [16], which is computationally more efficient in the polymer case. In a simulation, however, the director $\hat{n}(t)$ at time t is not an *a priori* known quantity. One therefore proceeds by computing the Saupe tensor [38],

$$Q_{\alpha\beta} = \frac{1}{N} \sum_{i=1}^N \left(\frac{3}{2} u_{i\alpha} u_{i\beta} - \frac{1}{2} \delta_{\alpha\beta} \right). \quad (4)$$

The sum runs over all bonds in the system. Q is a symmetric traceless tensor with the inversion symmetry of the nematic phase. The eigenvector for the largest of the three real eigenvalues $\langle \lambda_+ \rangle$ is the nematic director. The nematic phase is rotationally invariant around the director, so in this phase we have

$$\frac{1}{2} \langle \lambda_+ \rangle = - \langle \lambda_0 \rangle = - \langle \lambda_- \rangle, \quad (5)$$

where $\langle \lambda_0 \rangle$ denotes the middle and $\langle \lambda_- \rangle$ the smallest eigenvalue. In the isotropic phase we have

$$\langle \lambda_+ \rangle = \langle \lambda_0 \rangle = \langle \lambda_- \rangle = 0. \quad (6)$$

Defining $S = \langle \lambda_+ \rangle$ provides an equivalent way to calculate the nematic order parameter [36] which is generally used in computer simulations [37,39–41].

In a computer simulation the signature of a phase transition is always distorted by effects of the finite simulation volume. The magnitude of these effects depends on the ratio of the intrinsic length scale of the phenomenon (the correlation length ξ) to the linear system size L . This dependence has been used in the phenomenological finite size scaling theory [31,42], where the singular part of the free energy is written as a function of thermodynamic parameters such as the temperature and the ratio L/ξ . For the moments of the order parameter this leads to the well known [31,42] predictions at a second-order phase transition

$$\langle x^k \rangle(T, L) = L^{k\beta/\nu} \tilde{X} \left(T, \frac{L}{\xi} \right). \quad (7)$$

Here β is the order parameter critical exponent, ν characterizes the divergence of the correlation length at the critical point, $\xi \propto (T - T_c)^{-\nu}$, and \tilde{X} is a scaling function. It follows from Eq. (7) that exactly at T_c where $L/\xi = 0$, certain suitably chosen ratios of the order parameter moments $g_{2k} = \langle x^{2k} \rangle / \langle x^k \rangle^2$ are independent of the system size. The corresponding curves for different L as a function of temperature thus have a common intersection point at T_c . The most popular one of these ratios is the fourth-order cumulant

$$g_4 = \frac{\langle x^4 \rangle}{\langle x^2 \rangle^2}. \quad (8)$$

For reasons of statistical accuracy it is preferable, however, to work with the second-order cumulant [43]

$$g_2 = \frac{\langle x^2 \rangle}{\langle x \rangle^2}, \quad (9)$$

which is less susceptible to effects of statistical inaccuracy in the tails of the numerically generated order parameter distribution.

The cumulant intersection method can also be applied to first-order phase transitions [44–47]. Since the predictions for this case are different from those for second-order transitions, the method can serve as a tool to determine the order of the transition. For a first-order phase transition the phenomenological predictions are as follows [47].

(i) The curves of $g_4(T)$ for neighboring values of L intersect close to the transition temperature T_c , which means that the sequence of curves as a function of L at fixed T reverses at T_c . The intersection points $T_{cr}(L)$ converge to the critical temperature for $L \rightarrow \infty$,

$$\|T_{cr}(L) - T_c\| \propto L^{-2d}, \quad (10)$$

where d is the dimensionality of the system.

(ii) For small L the cumulant g_4 is a monotonically increasing function of T . For sufficiently large L , g_4 has a maximum in the disordered phase whose height scales as the volume and whose distance to the critical temperature scales as the inverse volume.

Quantitative predictions for the behavior of the second-order cumulant have not been derived so far, but qualitatively we expect a similar behavior. We will discuss our results for the second and fourth order cumulants in Sec. IV,

IV. RESULTS AND DISCUSSION

We have already seen qualitatively in Fig. 1 that our model exhibits a nematic ordering phenomenon for chain length $N=20$ at low temperatures. This can be seen very clearly when we look at the nematic order parameter S as a function of temperature in Fig. 4(a). This figure shows the nematic order parameter for several subsystem sizes of the simulation box of size $L=130$. We see a strong increase of the nematic order for temperatures below $T=0.27$, and the value of the order parameter becomes independent of the subsystem size at low temperatures. For higher temperatures any residual nematic order is clearly a finite size effect, as can be seen from the vanishing of the order parameter with increasing subsystem size. In contrast, we cannot observe such a phenomenon for the chain length $N=10$ in the same temperature interval [see Fig. 4(b)]. From this we cannot, however, exclude a transition for $N=10$ at considerably lower temperatures than those analyzed here. Due to the glassy freezing of the model at low temperatures, this problem is difficult to study.

Let us now turn to the determination of the phase transition temperature and the order of the transition for $N=20$. Figure 5(a) shows the fourth-order cumulant of the largest eigenvalue of the Saupe tensor as a function of temperature for different subsystem sizes, and Fig. 5(b) shows its second-order cumulant. Qualitatively we observe the predictions discussed in Sec. III. For small L the cumulants are monotonically increasing functions of temperature, whereas for larger L we see a peak occurring in the disordered phase. The arrows in the figures indicate intersection points of curves for neighboring L , and they appear to converge to a limiting value around $T=0.27$. There is, however, relatively large statistical

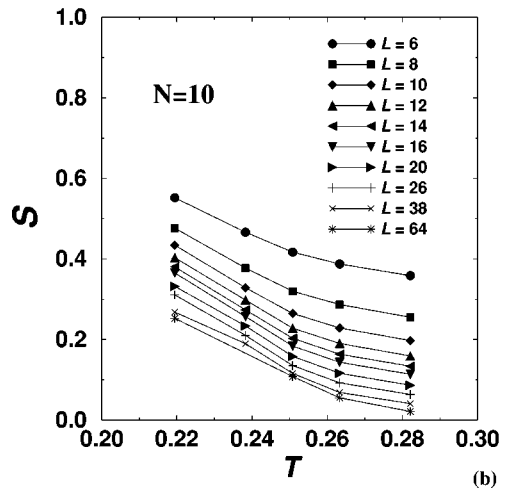
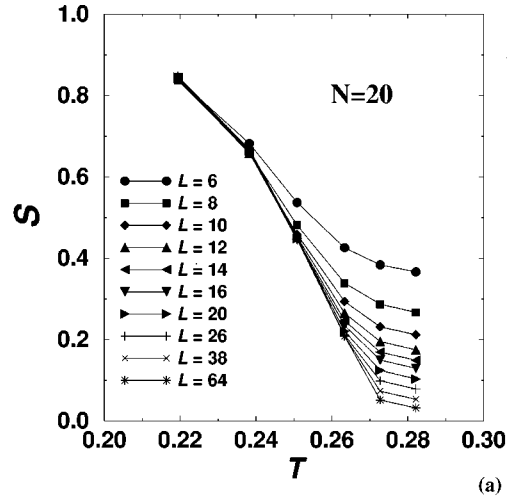


FIG. 4. (a) Nematic order parameter as a function of temperature for a melt of chains of length $N=20$. The different curves are for different subsystem sizes given in the legend. (b) Same as (a) for $N=10$.

scatter in the disordered phase, especially close to the peak position. As expected, the scatter is stronger for g_4 than for g_2 , but since the curves bundle up for large system sizes even for g_2 this scatter prevents a reliable determination of the intersection points of curves for different L 's when L becomes large. This also precludes an accurate extrapolation of the intersection points to the transition point.

The reason for this problem is the bundling up of the curves for different L 's in the disordered regime, which in turn stems from the finite size scaling behavior of the different moments $\langle \lambda_+^n \rangle$ of the order parameter. Figure 6 shows a comparison of the system size dependence of the largest and the middle eigenvalue of the Saupe tensor at $T=0.282$ in the disordered phase. For the moments of the largest eigenvalue, we observe a dependence approximately given by $\langle \lambda_+^n \rangle \propto L^{-nd/2}$, making g_2^+ and g_4^+ practically independent of the system size for large systems in the disordered phase. For the middle eigenvalue, however, the behavior is different. Here we find approximately $\langle \lambda_0^n \rangle \propto L^{-nd/2}$ for $n \geq 2$ but $\langle \lambda_0 \rangle \propto L^{-3}$. For a model system of uniaxial molecules this behavior was analytically predicted in Ref. [35]. As a consequence, the second-order cumulant of the middle eigenvalue should

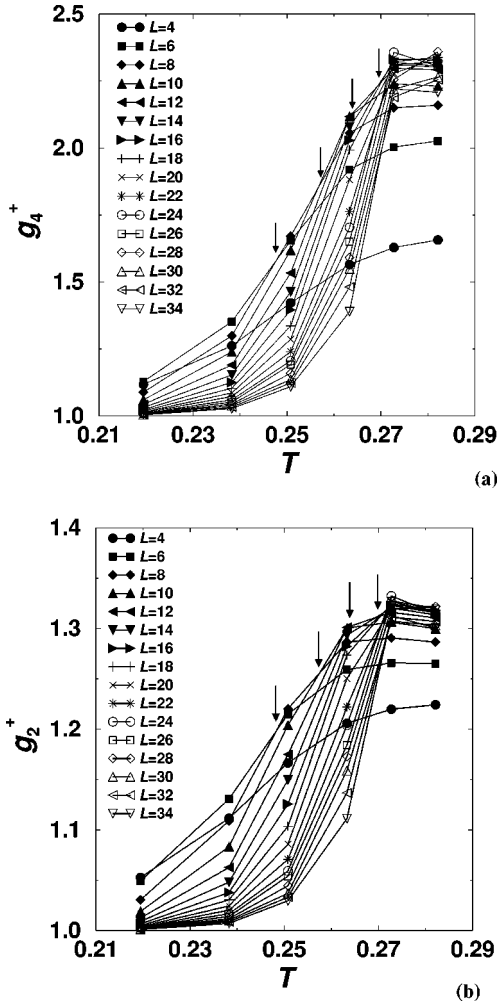


FIG. 5. (a) Fourth-order cumulant of the largest eigenvalue of the Saue tensor as a function of temperature. The different curves are for the subsystem sizes given in the legend. The arrows indicate intersection points of curves for neighboring subsystem sizes. (b) Same as (a) for the second-order cumulant of the largest eigenvalue of the Saue tensor.

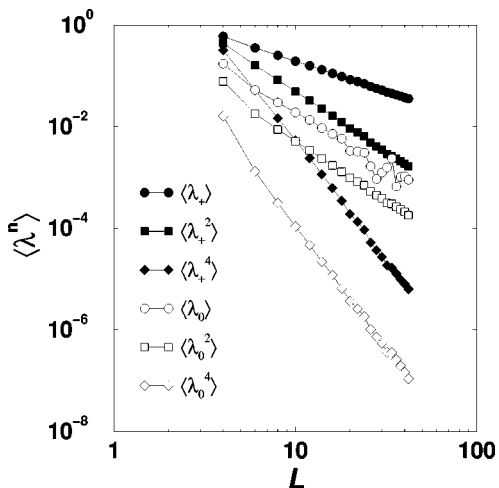


FIG. 6. System size dependence of the largest and the middle eigenvalue of the Saue tensor at temperature $T=0.282$ in the disordered phase. Note that $\langle \lambda_0 \rangle$ and $\langle \lambda_0^2 \rangle$ show the same slope.

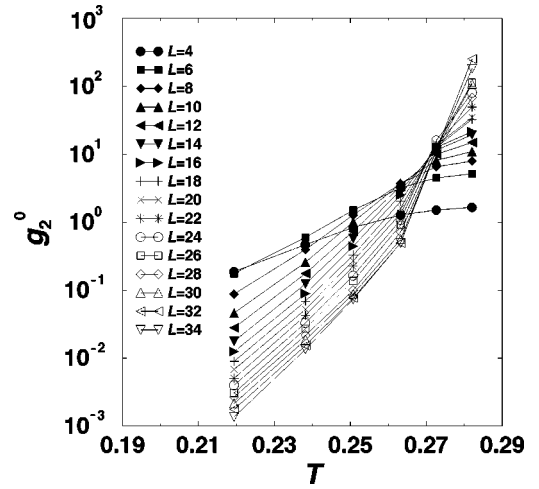


FIG. 7. Second-order cumulant of the middle eigenvalue of the Saue tensor as a function of temperature. The different curves are for the subsystem sizes given in the legend. Note that the curves for different subsystem size now show a marked system size dependence in the disordered phase.

scale as $g_2^0 \propto L^3$ in the disordered phase, thereby alleviating the problem caused by the bundling up of the curves. In Fig. 7 we show that this behavior indeed can be seen. Here the curves are sufficiently spread out so that it is possible with the accuracy obtainable in the simulation to determine the cumulant intersection points with sufficient precision. It may seem that the smallest subsystem linear dimension L included in our analysis (Figs. 5 and 7), $L=4$, is ridiculously small. However, an analysis of the orientational correlation function has revealed [32] a rather small value of the orientational correlation length ξ in the transition region, $\xi \approx 3$ lattice spacings. Thus our choice satisfies $L > \xi$. The resulting points are shown in Fig. 8 which presents the system size scaling of the cumulant intersection temperatures. The full curve is a fit with

$$T_{\text{cr}} = T_c - aL^{-3}. \quad (11)$$

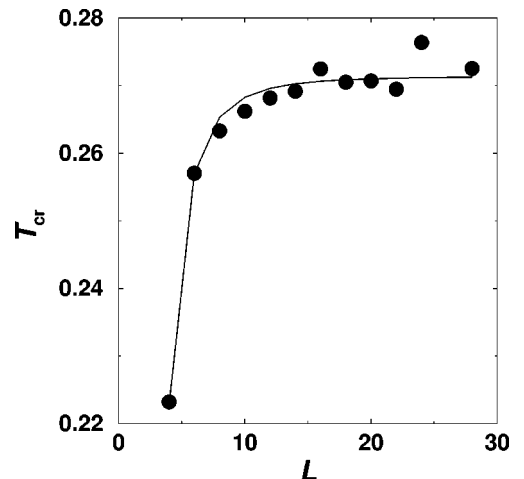


FIG. 8. Extrapolation to an infinite system size for the intersection temperatures of the second order cumulants in Fig. 7. The extrapolated first-order phase transition temperature is $T_c=0.271$.

The L^{-3} scaling would be expected for any first-order phase transition on general grounds [46,47]. From the fit we determined a transition temperature $T_c=0.271$ compatible with our prior estimates and a prefactor $a=3.11$.

In this way we are able to establish a first-order phase transition from a high temperature isotropic phase to the low temperature nematic phase in our model system of chains of length $N=20$. The transition is generated by the conformational changes in the chains which are forced toward the rigid rod ground state as the temperature decreases. The transition itself is entropy driven. The chains lose orientational entropy upon ordering, but they gain translational entropy. Since the Hamiltonian favors bonds of the type (2,0,0) in the rigid rod ground state there are, however, only three possible orientations each chain can take in its ground state on the simple cubic lattice. This small orientational entropy certainly increases the ordering tendency compared to a continuum simulation.

In comparison with earlier lattice simulations of different models, we can only speculate on why they failed to display an isotropic-nematic transition. There is always a competition between this transition and a glass transition in these simulations, when one increases the density at a fixed chain stiffness or the chain stiffness at a fixed density. When the density (stiffness) of the model at the isotropic-nematic transition is larger than the corresponding glass transition value, the phase transition is masked by the glassy freezing and is not observable in the simulation. The same Flory model [48] used for the mean-field treatment of the isotropic-nematic transition is also the basis of the Gibbs-DiMarzio theory [49] of the polymer glass transition. Also in our simulation, the self-diffusivity of chains at temperatures $0.35 < T < 0.6$ is compatible with a glassy freezing around $T=0.15$ [32]. However, even at the simulated density of $\phi=0.5$ the isotropic-nematic transition already occurs at a higher temperature (smaller stiffness), and is therefore observable in the simulation.

To gain further insight into the chain length dependence of this transition, we can try to interpret it in terms of the Onsager theory of the entropy driven isotropic-nematic transition [7,2] or the lattice model treatment of this transition by Flory [48,2]. For rigid rodlike polymers of length K and diameter d , both theories predict the limiting volume fraction of rods for the isotropic one-phase region to be

$$\phi^* = \text{const} \frac{d}{K}. \quad (12)$$

The value of the constant in the above equation is 3.29 for the numerical solution of the Onsager theory and 7.89 for the numerical solution of Flory's theory. In order to apply this equation to our simulation we equate the parameter d with the thickness of our chains ($d=2$), and the length of the rods with the square root of the mean squared end-to-end distance ($K=R_e = \sqrt{\langle R_e^2 \rangle}$). The latter relation is an exact identity in the ground state, and serves as a definition of the length for $T>0$. From the simulation we determined $\Phi^*=0.5$ for the

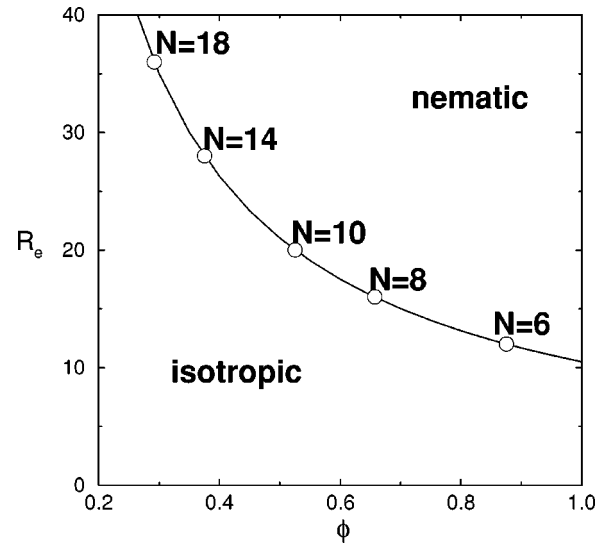


FIG. 9. Mean-field phase diagram according to the Onsager theory using the one determined transition point ($\Phi=0.5, R_e=21$). The opaque circles indicate the volume fractions where the respective chain lengths would just show a zero temperature phase transition to the nematic phase.

temperature $T=0.271$. At this temperature we find $\langle R_e^2 \rangle(T=0.271)=440.62$. This gives an empirical value of $\text{const}=5.25$ for the constant in Eq. (12), which lies between the values for the continuum and the simple lattice model that Flory studied. We can now plot an approximate transition line in the (ϕ, R_e) plane, which is given by

$$R_e = \frac{10.5}{\phi}. \quad (13)$$

The resulting phase diagram is shown in Fig. 9 for $0.2 < \phi < 1$, where the full line denotes the stability limit ϕ^* of the isotropic phase. For fixed volume fraction of the simulation we expect a phase separation into an isotropic phase with a density given by the curve, and a nematic phase at a higher density as soon as R_e becomes larger than $10.5/\phi$. Also included are transition points for chain lengths $N=6-18$ for temperature $T=0$, where the length of the chains in their rigid rod ground state is $R_e=2N$, and the transition density is $5.25/N$. From this diagram we conclude that at a volume fraction in the simulation of $\phi=0.5$ all chains of length $N > 10$ should show an isotropic-nematic phase transition at some temperature $T>0$. The chains of length $N=10$ for which the order parameter was shown in Fig. 4(b) are therefore not expected to order at the simulation density.

ACKNOWLEDGMENTS

H.W. acknowledges funding through a EU Joint Research Project under Grant No. CIPA-CT93-0105. The study was made possible by generous grants of computing time at the Zentrum für Datenverarbeitung, University of Mainz, and the Regionale Hochschulrechenzentrum Kaiserslautern.

- [1] P. J. Collings, *Liquid Crystals* (Hilger, Bristol, 1990).
- [2] *Liquid Crystallinity in Polymers*, edited by A. Ciferri (VCH, New York, 1991).
- [3] P. G. de Gennes and J. Prost, *The Physics of Liquid Crystals*, 2nd ed. (Clarendon, Oxford, 1992).
- [4] G. J. Vroege and H. N. W. Lekkerkerker, *Rep. Prog. Phys.* **55**, 1241 (1992).
- [5] W. Maier and A. Saupe, *Z. Naturforsch. A* **13**, 564 (1958).
- [6] M. M. Telo da Gama, in *Observation, Prediction and Simulation of Phase Transitions in Complex Fluids*, edited by M. Baus, L. F. Rull, and J.-P. Ryckaert (Kluwer, Dordrecht, 1995).
- [7] L. Onsager, *Ann. (N.Y.) Acad. Sci.* **51**, 627 (1949).
- [8] J. R. McColl and C. S. Shih, *Phys. Rev. Lett.* **29**, 85 (1972).
- [9] M. Ballauf, in *Observation, Prediction and Simulation of Phase Transitions in Complex Fluids* (Ref. [6]).
- [10] A. R. Khokhlov and A. N. Semenov, *Physica A* **108**, 546 (1981); **112**, 605 (1982).
- [11] T. Odijk, *Macromolecules* **19**, 2313 (1986).
- [12] R. Hentschke, *Macromolecules* **23**, 1192 (1990); R. Hentschke and J. Herzfeld, *Phys. Rev. A* **44**, 1148 (1991).
- [13] D. B. DuPré and S.-j. Yang, *J. Chem. Phys.* **94**, 7466 (1991).
- [14] Z. Y. Chen, *Macromolecules* **26**, 3419 (1993).
- [15] M. R. Wilson and M. P. Allen, *Mol. Phys.* **80**, 277 (1993).
- [16] M. Dijkstra and D. Frenkel, *Phys. Rev. E* **50**, 349 (1994); **51**, 5891 (1995).
- [17] P. J. Flory, *Proc. R. Soc. London, Ser. A* **234**, 60 (1956).
- [18] P. D. Gujrati, *J. Phys. A* **13**, L437 (1980); P. D. Gujrati and M. Goldstein, *J. Chem. Phys.* **74**, 2596 (1981).
- [19] A. I. Milchev, *C. R. Acad. Bulg. Sci.* **36**, 1415 (1983).
- [20] H. P. Wittmann, *J. Chem. Phys.* **95**, 8449 (1991).
- [21] M. Wolfgang, J. Baschnagel, W. Paul, and K. Binder, *Phys. Rev. E* **54**, 1535 (1996).
- [22] A. Baumgärtner, *J. Chem. Phys.* **84**, 1905 (1986).
- [23] A. Kolinski, J. Skolnick, and R. Yaris, *Macromolecules* **19**, 2560 (1986).
- [24] J. F. Nagle, *Proc. R. Soc. London, Ser. A* **337**, 569 (1974).
- [25] A. Malakis, *J. Phys. A* **13**, 651 (1980).
- [26] H.-P. Deutsch and K. Binder, *J. Chem. Phys.* **94**, 2294 (1991); H.-P. Wittmann and K. Kremer, *Comput. Phys. Commun.* **61**, 309 (1990); W. Paul, K. Binder, D. W. Heermann, and K. Kremer, *J. Phys. II* **1**, 37 (1991).
- [27] K. Binder and W. Paul, *J. Polym. Sci., Part B: Polym. Phys.* **35**, 1 (1997).
- [28] The parameters in the Hamiltonian came from a mapping procedure of a realistic polymer model onto the bond-fluctuation lattice model [W. Paul and N. Pistor, *Macromolecules* **27**, 1249 (1994)], but in this context it is only their property of generating an intramolecular transformation from a Gaussian coil into a rigid rod upon cooling that is of importance.
- [29] H. Weber and W. Paul, *Phys. Rev. E* **54**, 3999 (1996).
- [30] H. Weber, W. Paul, W. Kob, and K. Binder, *Phys. Rev. Lett.* **78**, 2136 (1997).
- [31] K. Binder, *Z. Phys. B* **43**, 119 (1981).
- [32] H. Weber, dissertation, Institut für Physik, Johannes-Gutenberg Universität Mainz, 1997 (unpublished).
- [33] V. Tries, W. Paul, J. Baschnagel, and K. Binder, *J. Chem. Phys.* **106**, 738 (1997).
- [34] D. Frenkel and B. M. Mulder, *Mol. Phys.* **55**, 1171 (1985).
- [35] R. Eppenga and D. Frenkel, *Mol. Phys.* **52**, 1303 (1984).
- [36] M. P. Allen, G. T. Evans, D. Frenkel, and B. M. Mulder, *Adv. Chem. Phys.* **86**, 1 (1993).
- [37] M. P. Allen, in *Observation, Prediction and Simulation of Phase Transitions in Complex Fluids*, edited by M. Baus, L. F. Rull, and J.-P. Ryckaert (Kluwer, Dordrecht, 1995).
- [38] A. Saupe, *Z. Naturforsch. A* **19A**, 161 (1964).
- [39] R. D. Mountain and T. W. Ruijgrok, *Physica A* **89**, 522 (1977).
- [40] C. Zannoni, in *The Molecular Physics of Liquid Crystals*, edited by C. R. Lockhurst and G. W. Gray (Academic, London, 1979).
- [41] G. J. Zarragoicoechea, D. Levesque, and J. J. Weis, *Mol. Phys.* **75**, 989 (1992).
- [42] K. Binder, in *Finite Size Scaling and Numerical Simulations of Statistical Systems*, edited by V. Privman (World Scientific, Singapore, 1990); D. P. Landau, *ibid.*
- [43] H.-P. Deutsch, *J. Stat. Phys.* **67**, 1039 (1992).
- [44] K. Binder and D. P. Landau, *Phys. Rev. B* **30**, 1477 (1984).
- [45] M. S. S. Challa and D. P. Landau, *Phys. Rev. B* **33**, 437 (1986).
- [46] M. S. S. Challa, D. P. Landau, and K. Binder, *Phys. Rev. B* **34**, 1841 (1986).
- [47] K. Vollmayr, J. D. Reger, M. Scheucher, and K. Binder, *Z. Phys. B* **91**, 113 (1993); K. Vollmayr, Diploma thesis, University of Mainz, 1992 (unpublished).
- [48] P. J. Flory, *Proc. R. Soc. London, Ser. A* **234**, 73 (1956).
- [49] J. H. Gibbs and E. A. Di Marzio, *J. Chem. Phys.* **28**, 373 (1958); **28**, 807 (1958).